USING COATING ROUGHNESS TO CONTROL PIPE-SOIL FRICTION AND INFLUENCE PIPELINE GLOBAL BUCKLING BEHAVIOUR

Lawrence W. de Leeuw, University of Bristol, Bristol, UK, lawrence.deleeuw@bristol.ac.uk
Andrea Diambra, University of Bristol, Bristol, UK, Andrea.Diambra@bristol.ac.uk
Matthew S. Dietz, University of Bristol, Bristol, UK, M.Dietz@bristol.ac.uk
Henry Milewski, TechnipFMC, Westhill, UK, henry.milewski@technipfmc.com
George Mylonakis, University of Bristol, Bristol, UK, g.mylonakis@bristol.ac.uk
Oh-Sung Kwon, University of Toronto, Toronto, Canada, os.kwon@utoronto.ca
Anastasios G. Sextos, University of Bristol, Bristol, UK, a.sextos@bristol.ac.uk

ABSTRACT

Submarine on-bottom High Pressure / High Temperature pipelines are susceptible to buckling and walking phenomena to relieve axial stress built up in the pipeline through thermal expansion. Axial stress is dependent on the friction coefficient between seafloor soils and pipeline coatings and has a controlling influence on the instigation of buckles. Typical approaches to controlling the formation and distribution of buckles is the placement of sleepers or sliders to promote or discourage lateral deformation. Herein, an alternative methodology is proposed where variation of the pipe-soil interaction friction coefficient axially can promote analogous behaviour. Recent experimental investigations have characterised friction coefficients for polypropylene, a typical pipe coating material, with typical real-world surface textures and also with enhanced textures designed to improve interface shear strength. Finite element analysis using Abaqus was used in this paper to model an approximately 5 km on-bottom pipeline subject to operational loads typical of HPHT systems. The results show that pipe-soil friction has the expected impact on axial stress build up and buckle properties, but also that axial variation of PSI friction can be an effective method for influencing the distribution of buckle formation.

Keywords: pipelines, buckling, pipe-soil interaction, numerical analysis

INTRODUCTION

Hydrocarbon exploration and extraction is taking place in increasingly deep waters as previously unavailable reserves become accessible through engineering improvements and socio-economic imperatives. A consequence of geologically deeper reservoirs is that reservoir temperatures and pressures are greater. High Pressure High Temperature (HPHT) reservoirs, typically considered to be greater than 69 MPa and 150°C (Shadravan and Amani, 2012), lead to commensurately greater operating loads for pipelines supporting the oil field.

HPHT pipelines are vulnerable to Euler column buckling due to their length and slenderness. A range of methods have been adopted or are proposed to control pipe motions. Solutions generally involve adding additional infrastructure to increase the weight of pipelines with rock dump, concrete mattress, or anchors to increase shearing resistance or provide physical restraint on motion. Some techniques adopt the opposing approach with the use of sliders or increasing buoyancy to reduce shearing resistance or create a "vertical upset" (Bruton et al., 2005) so that buckling can be promoted at a location of the designer's choosing. An alternative philosophy to global pipeline stability is to control or influence buckling by pre-determining as-laid pipeline geometry. Pipe geometry solutions such as snake-lay (Perinet and Frazer, 2006) and continuous sinusoidally pre-deformed pipe (Chee et al., 2018) have been shown to reduce axial force build-up and more evenly distribute lateral deformation along the length the pipe leading to lower overall magnitudes of displacement.

Axial stress in the pipe wall builds up because the thermal expansion of the pipe is restrained by the resistance offered by the soil along the pipe-soil interface. The frictional component of pipe-soil interaction plays a crucial role in global pipeline stability with direct influence on axial force build-up, resistance to pipe walking, and lateral buckling. Unfortunately, pipeline stability design often has conflicting requirements from PSI friction as noted by White and Tian (2014) and Milewski et al. (2019). High pipe-soil interface friction offers greater resistance to route curve pull out, lateral buckling breakout, and pipe end expansion but also leads to a greater rate of build-up of axial force.

Conversely, low pipe-soil interface friction means a lesser build-up of axial force but also reduces the resistance to formation of buckles.

Pipelines are typically given a protective coating to provide protection from corrosion, damage during transit and operation, and to thermally insulate the pipeline. A common coating material is polypropylene and as it forms the outer pipe surface, correct quantification of polypropylene-soil friction parameters is key to robust pipeline stability design. Recent experimental work quantifying polypropylene interface strength with granular soils at stresses relevant to pipelines has revealed interface friction factors show a strong dependency on surface roughness and grain size (De Leeuw *et al.*, 2019; Milewski, *et al.*, 2019; De Leeuw *et al.*, 2020). Milewski *et al.* (2020) show that polypropylene surfaces can be roughened, and enhanced textures lead to greater interfacial friction related to a relationship dependent on the surface roughness and average grain size. The possibility to engineer a surface texture and specify an interface friction coefficient depending on the substrate grain size provides intriguing possibilities for improving pipeline stability design and performance.

This research draws on experimental pipe-soil interface shear strength data and uses Abaqus general purpose finite element software to study the possibility of improving pipeline design using engineered surface roughness. Interestingly, such pipe-soil friction control can also be implemented to reduce axial strains at geotechnical discontinuities of onshore pipes during seismic events (Psyrras *et al.*, 2018). It is hoped that quantifying and controlling a surface roughness prior to pipe-laying can provide a viable alternative to other previously discussed buckling mitigation or design techniques, potentially reducing construction and maintenance costs associated with ship time and multiple voyages to install secondary infrastructure.

EXPERIMENTAL BASIS

A large number of interface shear tests were carried out using a modified Direct Shear Apparatus to quantify polypropylene-soil interface shear strength (De Leeuw *et al.*, 2020) and to investigate the impact of surface roughness on interface strength (Milewski, *et al.* 2020). Surfaces were roughened using a combination of laser-engraving techniques, sandblasting, and embossing with a knurled surface. The roughening techniques may not be exactly replicable on an industrial scale, but alternatives could be implemented and incorporated during manufacturing. Some data from De Leeuw *et al.* (2020) showing the friction coefficients between real pipe specimens and various soils, and from Milewski *et al.* (2020) with enhanced roughness surfaces, are presented in Figure 1. It is assumed that interface shear strengths are applicable to pipe-soil interface acting in both axial and lateral directions. Soil parameters, particle size distributions (PSDs) and further details about the experimental work, are provided in Milewski *et al.* (2020) in these proceedings.
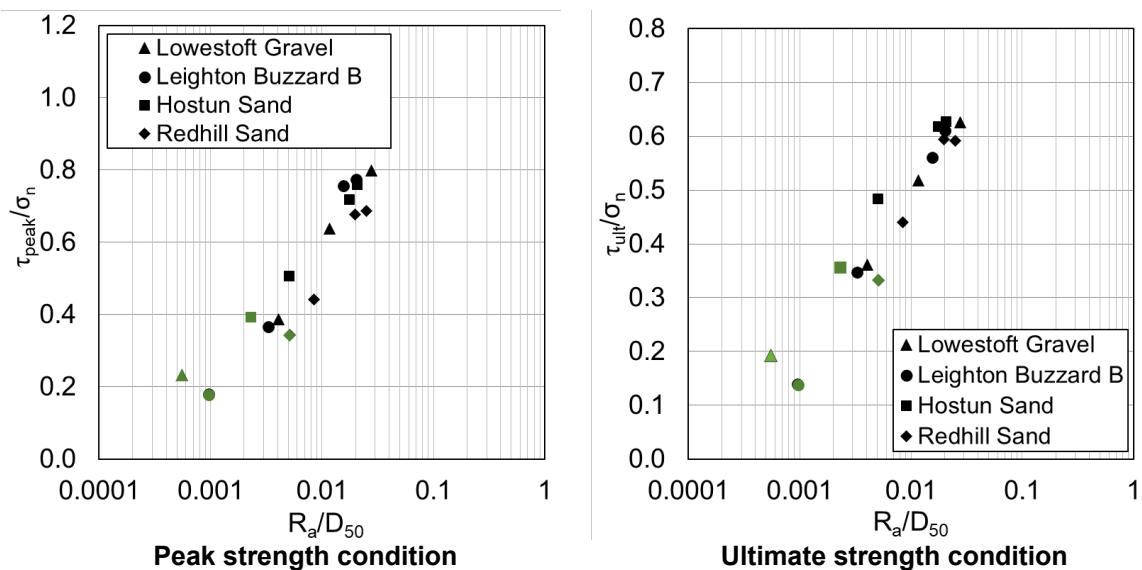

Peak strength condition   **Ultimate strength condition**

Fig. 1. Interface friction coefficient at σ_n = ~20kPa, D_r = ~70% varying with relative roughness. Green points represent real polypropylene coating specimens after De Leeuw *et al.* (2020). Black points are enhanced roughness specimens after Milewski *et al.* (2020).

It can be seen in Figure 1 after that the large displacement (ultimate) friction coefficients for real pipe specimens (green data points) fall in the range of 0.15 to 0.35. Enhancing the surface texture (achieved here variously by laser engraving and sandblasting) resulted in a large increase in friction coefficient (for both peak and ultimate conditions). Friction coefficients of up to 0.62 were achieved for ultimate conditions representing a large potential range of friction coefficients available to pipeline designers. Soil dilatancy and the mobilisation of peak strengths like soil-only behaviour also offers possibilities for enhanced initial breakout resistance.

NUMERICAL ANALYSIS

The range of friction coefficients shown in Figure 1 have informed the range investigated in the present study. Friction coefficients of 0.25, 0.50, and 0.75 were investigated, applied both uniformly and differentially along the pipe to study the impact on buckling response. There is significant precedent in FE modelling of pipelines for the use of Abaqus general purposes finite element analysis (Jukes *et al.*, 2008; Jukes *et al.*, 2009; Cumming *et al.*, 2009; Cumming and Rathbone, 2010; Jin *et al.*, 2010; Bruton *et al.*, 2011; Sun *et al.*, 2011; Liu *et al.*, 2014; Chee *et al.*, 2018, Psyrras *et al.*, 2018). Abaqus is well suited to the modelling pipelines as it incorporates pipe-type beam elements, pipe-soil interaction mechanisms, can accommodate large displacements and model dimensions, and can model highly non-linear behaviour.

Model case study

Modelling parameters for this research are adapted from Chee *et al.* (2018) who reported a typical example of a pipeline which may be laid by conventional methods, e.g. S-lay or reel-lay. Pipe properties and modelling parameters are summarised in Table 1.

Table 1 Modelling parameters

| Parameter	Unit	Value
Pipe outside diameter (OD)	m	0.3556
Pipe wall thickness (WT)	m	0.0198
Pipe submerged weight, W_s	kN/m	0.61
Pipeline total length, L_t	m	4880
Maximum operating temperature, T_{op}	°C	200
Ambient temperature, T_{amb}	°C	0
Maximum operating pressure, P_{op}	kPa	20,000
Pipeline steel Young's Modulus, E	kPa	2.05e08
Coefficient of steel thermal expansion, α	1/°C	1.3e-05
Pipeline steel (bilinear) yield stress / strain	-	448 MPa / 0.02 and 530 MPa / 0.13
Pipe-soil friction coefficient, μ	-	0.25 / 0.50 / 0.75 / variable

Pipe model

The pipeline was modelled using PIPE31H beam-type elements which are 3D two-node linear pipe elements with 6 degrees-of-freedom at each node and numerical integration of material response at 32 integration point around the circumference. Transverse shear deformation is allowed by a Timoshenko beam formulation and the hybrid formulation improves convergence where axial stiffness is much greater than bending stiffness. These formulations are particularly useful where the pipeline is likely to undergo large rotations when buckling. The pipe model was meshed to give 1 m length pipe elements.

Pipe-soil interaction

The seabed was modelled as a horizontal, flat, hard surface by using C3D20R elements with very high material property elastic stiffness and the whole element declared to be rigid. Contact pairs were used to model the interaction between pipe and seabed, using node-to-surface contact with the seabed as the master surface. Interaction behaviour was modelled using hard contact and the friction penalty method to provide the equivalent friction coefficient for large-displacement, ultimate strength conditions. Where appropriate, peak frictional behaviour, the effect of pipe embedment,

and passive resistance offered by soil berms was modelled with the application of supplementary non-linear springs active over the appropriate initial displacements in the lateral direction only. Initially the force-displacement model of Chee *et al*. (2018) was used to validate the model against their work. For the differential friction models shown in Figure 6 the force-displacement model was determined from the analytical solution for calculating passive resistance proposed by Verley and Sotberg (1994) assuming an initial pipe embedment of 5% of the pipe outside diameter. Real world pipe embedment may be greater and is likely to have an impact on the nature of global buckling response. The force-displacement responses adopted for this research are shown in Figure 2 which presents results of a displacement control test used to validate the pipe-soil interaction frictional model. Friction coefficient, μ, was applied to the axial direction and the combined μ + nonlinear spring response was applied to the lateral direction.

(a) **After Chee *et al*. (2018)**   (b) **After Verley and Sotberg (1994)**
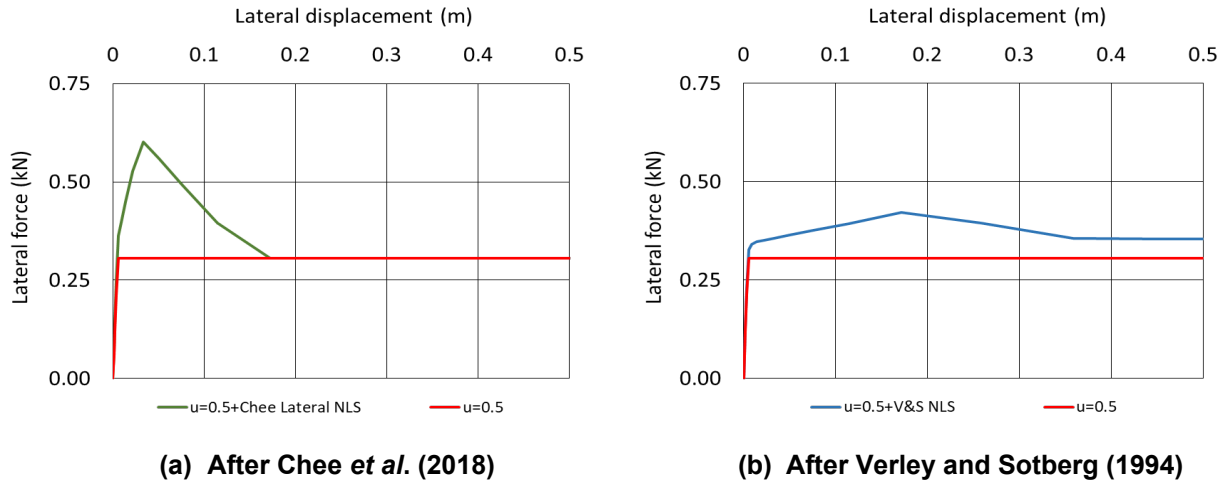
Fig. 2. Results of a displacement control test with a single element in Abaqus to validate the force-displacement response of the pipe-soil interaction model after Chee *et al*. (2018) and Verley and Sotberg (1994).

Loading

The total submerged weight of the operational pipe was accounted for by applying a uniformly distributed line load to the pipe elements. Initial temperature was assumed to be 0°C with temperature loading calculated by Abaqus using the imposed change in temperature and the coefficient of linear thermal expansion as defined in Table 1. Initial internal pressure was considered to be 0 kPa and during loading steps temperature and pressure were applied simultaneously. Initial external pressure was not considered because it does not change during pipe operation.

Assumptions

A number of assumptions were made to aid simplicity, improve computational efficiency, and to focus on the pipe-soil friction coefficient as the variable of interest. The soil elements were declared to be stiff, flat, and rigid to prevent any embedment or deformation of the contact surface and no provision was made for uneven seabed topography. Linear elastic springs acted laterally and axially on the pipe ends with a spring stiffness of 100 kN/m to simulate typical resistance offered by end expansion spools as in Chee *et al*. (2018). Non-linear springs resisting lateral pipe movement act with reference to the global coordinate system which means that in effect their directionality may not always be perfectly perpendicular to the pipe if the pipe is subject to deformation. This discrepancy was not considered to be problematic as deviations from perfectly perpendicular were relatively small due to the length over which lateral deformations occur.

Boundary Conditions

The model was run in two steps, the first to apply the self-weight of the pipe and the second to simultaneously apply the pipe internal pressure and the temperature field to the pipe only. During application of the self-weight, boundary conditions were set to allow only vertical movement of the pipe. During the loading step, all boundary conditions were removed from the pipe such that the only

forces acting on it were the pipe pressure load, strain generated by the temperature field, and the reaction forces of the springs modelling end expansion spools or soil response. For each stage the seabed element remained rigid.

COMPARATIVE STUDY

To benchmark this research the model was produced to replicate the results of Chee *et al*. (2018) to validate the present work. In this research a simple friction penalty method was used between pipe and seafloor to mimic Mohr-Coulomb frictional behaviour, adopting 0.50 as the friction coefficient which means that 0.50 of the normal force is available to mobilise as a shear resistance force. Additional lateral-only non-linear springs were added to mimic the nonlinear response of breakout and passive soil resistance. The force-deformation relationship is shown in Figure 2 and is the same as in Chee *et al*. (2018).

Perfect pipe geometry

Initial pipe geometries were defined to be perfect in their geometrical arrangement. Model outputs for effective axial force, lateral position along the pipeline are presented in Figure 3 for perfectly straight and perfectly Pre-deformed Pipe (PDP) at 50% and 100% of maximum operating loads after Chee *et al*. (2018). The results show very good agreement between the model outputs of the current study with those of the benchmark study. The pipe ends show effective axial forces that are non-zero due to the reaction force of the pipe end spring stiffness imposed to model end expansion spools.
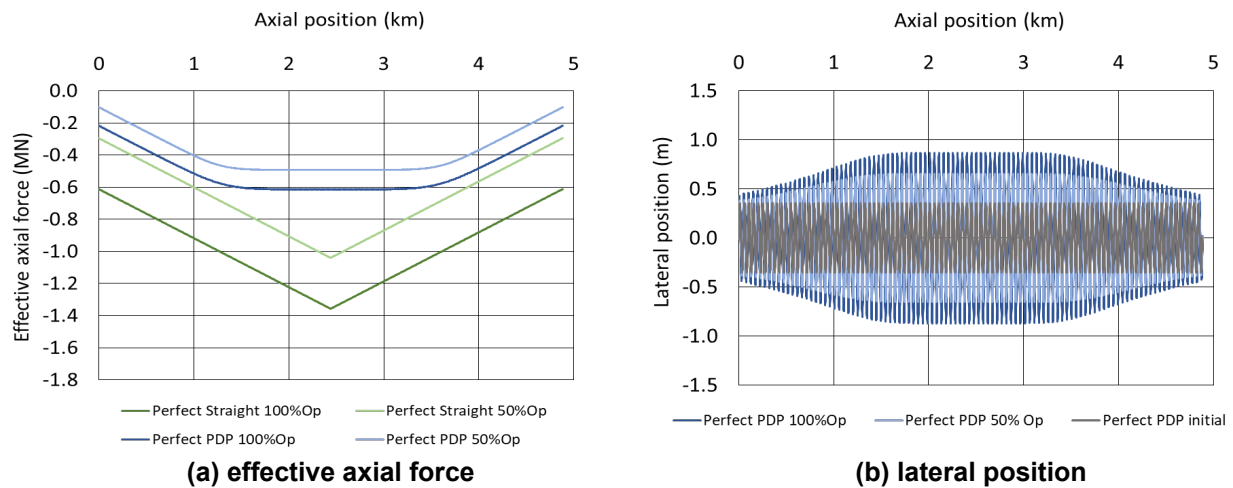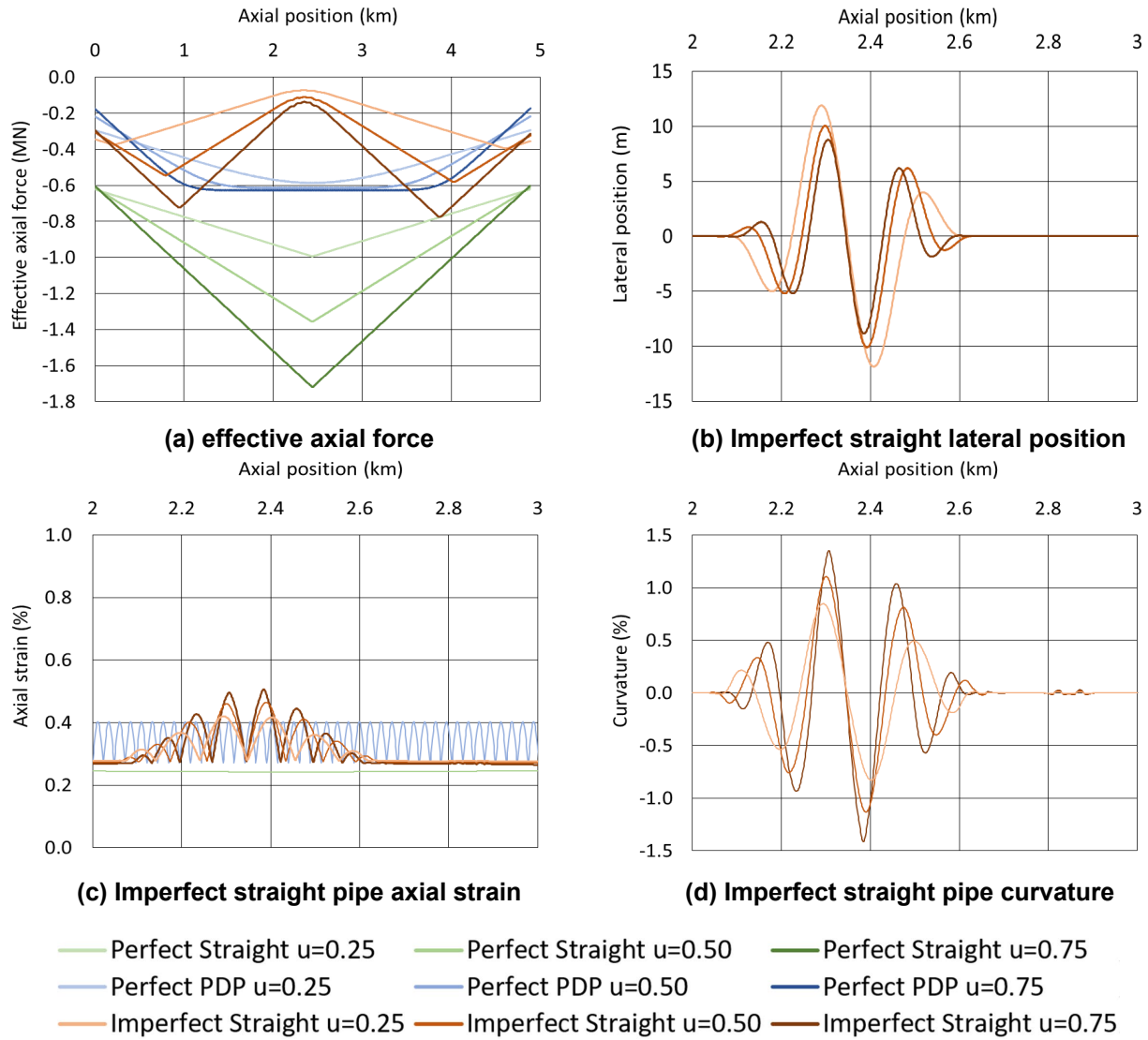

(a) effective axial force **(b) lateral position**

Fig. 3. Effective axial force and lateral position at operating load for perfect straight and PDP pipe.

Imperfect pipe geometry

In reality, pipe geometry will never be perfect. Even with the dubious assumption that the pipeline itself is perfectly homogenous, variation in seafloor topography and initial out-of-straightness from pipe laying is likely to lead to subtle geometric variations from the ideal. To capture this variability Chee *et al*. (2018) introduced randomised imperfections to the pipe as-laid geometry (note, not the pipe section or structural imperfections). Variations from the idealised perfect positions of up to ±0.1m were assumed to occur along the pipe. The distribution and exact magnitude of the above imperfections was determined by random number generation. It is not possible to directly compare the results for imperfect pipe geometries against those of Chee *et al*. (2018) because the geometries are essentially different.

FRICTION PARAMETRIC STUDY

Three pipe geometries (perfect straight, perfect PDP, and imperfect straight) were analysed with varying friction coefficients and the results for effective axial force, and axial strain, curvature, and lateral displacement of the single central buckle that formed with imperfect straight pipe are shown in Figure 4.

(a) effective axial force

(b) Imperfect straight lateral position

(c) Imperfect straight pipe axial strain

(d) Imperfect straight pipe curvature

Legend:
Perfect Straight u=0.25 — Perfect Straight u=0.50 — Perfect Straight u=0.75
Perfect PDP u=0.25 — Perfect PDP u=0.50 — Perfect PDP u=0.75
Imperfect Straight u=0.25 — Imperfect Straight u=0.50 — Imperfect Straight u=0.75

Fig. 4. (a) effective axial force and (b) lateral position of imperfect straight pipe along the length of the pipeline with varying ultimate friction coefficients of 0.25, 0.50, and 0.75, (c) axial strain and (d) curvature for the imperfect straight pipe.

Considering first the effective axial force shown in Figure 4a, the slope of the line is equal to the axial pipe-soil resistance, i.e. the self-weight of the pipe multiplied by the friction coefficient. It is clear that reduced friction coefficients lead to a lesser build-up of effective axial force which is best illustrated in green for the perfect straight pipe although this is unrealistic in practise. Chee *et al.*'s (2018) perfect PDP pipe reaches the same constant value at a rate dependent on the friction coefficient and results in lateral deformations of equal magnitude (not explicitly shown here) as shown in Figure 3b. Straight pipe with initial random imperfections shows a tendency for a single large lateral deformation at the mid-point shown in Figure 4b. It is clear to see that lower pipe-soil friction leads to greater global buckle amplitude and also leads to a subtle extension and change in the buckle form with respect to axial position. Axial strain and curvature vary also with friction coefficient with the tighter buckles of higher friction corresponding to greater curvature These trends are expected and consistent with current understanding of global buckling.

Table 2 Pipe end expansion

Pipe geometry	Chee et al. (2018)	u = 0.25	u = 0.50	u = 0.75
Perfect Straight	6.1m	6.2m	6.1m	6.0m
Perfect PDP	2.1m	2.9m	2.2m	1.7m
Imperfect Straight	unknown	3.5m	3.2m	3.0m

A third limit state to consider is expansion at pipe ends. Table 2 summarises the end expansions reported by Chee *et al*. (2018) and those determined from the present study. Friction coefficient of 0.50 most closely matches Chee *et al*. (2018) model parameters. Additionally, the influence of friction coefficient shows the expected trend of greater friction suppressing end axial displacement.
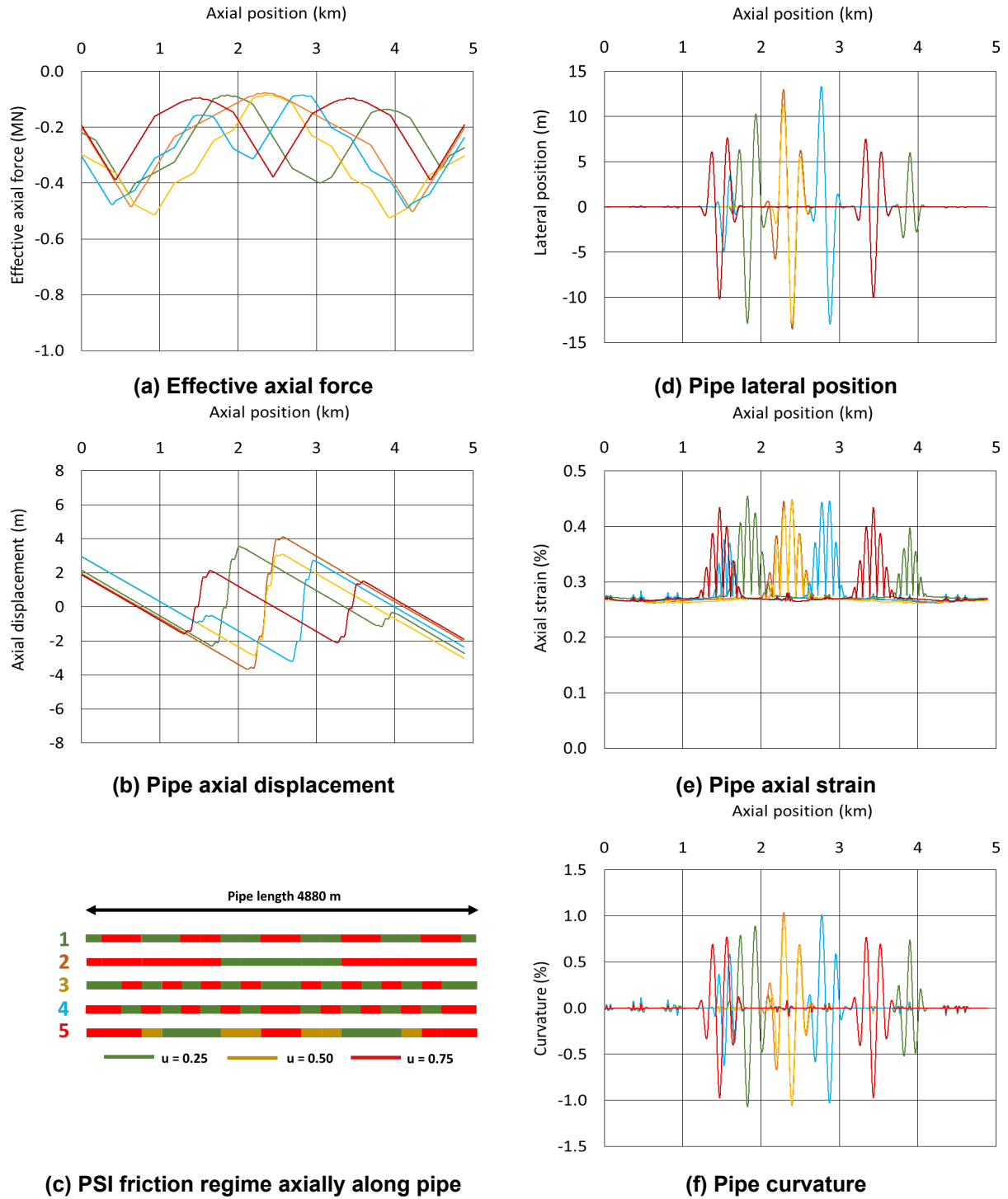
DIFFERENTIAL PSI FRICTION

There are two aspects of pipe-soil friction modification that require consideration. The first is that the above results are from a pipe model which assumes a pipe of uniform interface friction on a uniform seabed. In reality, as shown in Figure 1, the interface friction coefficient is a function of both surface properties and substrate grain size. Figure 5 shows the distribution of oil and gas pipelines across the North Sea basin and also the distribution of sediment type. Considering Figures 1 and 5 it can be easily envisaged that a very long pipe will experience different pipe-soil friction conditions along its length without any change to surface coating texture. Control of surface textures could be used to compensate for unfavourable PSI conditions where pipelines cross very variable seabeds. As previously mentioned, such techniques have been found to be useful as mitigation measures for maintaining gas pipeline integrity over soil discontinuities in earthquake regions. It is considered a key parameter for enhancing the stability of pipelines against phenomena that induce axial strain (seismic waves, thermal expansion).
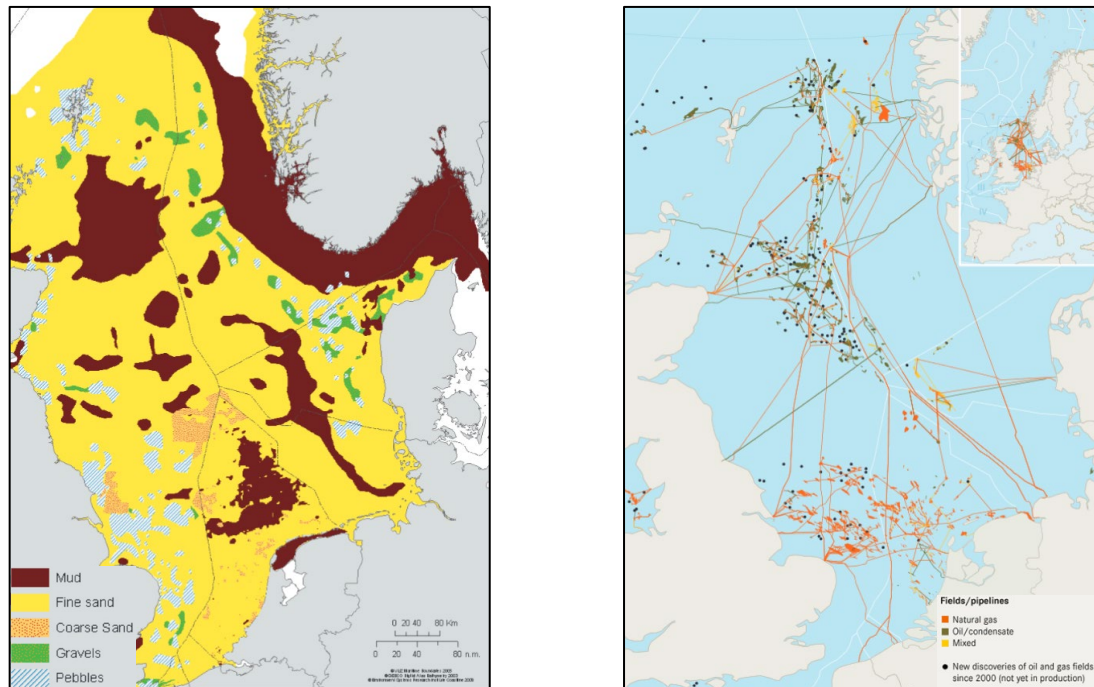
Fig. 5. Substrate map of North Sea basin from MEFEPO (Paramor, 2009) and map of oil and gas pipeline routes across the North Sea from oil field to terrestrial terminals from OSPAR (2010).

The differences in pipeline stability performance with different PSI friction and the potential for engineering surface texture during the manufacturing process invites the possibility of applying coatings with differential friction along the pipeline. Patterns of pipe coating or targeting control of friction where seabed conditions might otherwise be unfavourable, gives potential for pipeline global stability to be controlled in ways other than by use of secondary infrastructure. In this preliminary study, a number of arrangements for PSI friction coefficient varying along the length of the pipeline were modelled using the "imperfect straight" pipeline geometry. Results of friction coefficient variations axially along the pipe are presented in Figure 6 and can be compared directly with the uniform friction regimes shown in Figure 4 as the initial pipe geometries are identical. The variation in PSI friction along the pipe for each configuration is presented to scale in Figure 6 such that direct comparison between friction configuration and pipe response can be made. Different friction coefficients are colour coded according to the legend and each configuration given a coloured number corresponding to the colour scheme used in the plots.

(a) Effective axial force

(b) Pipe axial displacement

(c) PSI friction regime axially along pipe

(d) Pipe lateral position

(e) Pipe axial strain

(f) Pipe curvature

Fig. 6. Distribution and magnitude of global stability parameters (a) effective axial force, (b) axial displacement, (d) lateral position, (e) axial strain, (f) pipe curvature, with different PSI friction regimes varying along the pipe (c).

Comparison of Figures 4 and 6 reveals a dramatic change in the distribution and magnitude of buckles formation. Under the single PSI friction regime Figure 4 shows that for an imperfectly straight pipe, a single global buckling feature occurs at the mid-point accompanied with the expect decrease in effective axial force at that point. A similar response is seen in configurations 2 and 3 in Figure 6 and examination of the PSI regime imposed shows a low friction area in the central zone. Configurations 1, 4, and 5, where the mid-point of the pipe has a greater friction coefficient than elsewhere, leads to the formation of two buckles instead of one and they are distributed away from the mid-point by varying amounts depending on the detail of the PSI friction regime.

Differences in end expansion over the relatively short pipeline length modelled appear to be quite modest, though in percentage terms they vary significantly. Average end expansion for each friction regime can be determined from the axial displacement plot of Figure 6b. Generally, end expansion magnitudes are less than determined using a single PSI friction and are of comparable magnitude to Chee *et al.*'s (2018) PDP geometry.

SUMMARY AND CONCLUSIONS

A numerical study of unburied offshore pipelines was undertaken. Changes in PSI friction show the expected impact on pipeline global stability effects and it has been shown that axial variation of PSI friction regimes can allow the designer to influence the distribution of buckle formation. Use of differential PSI friction through engineering surface textures could provide a useful additional dimension to methods of controlling pipeline global stability.

ACKNOWLEDGMENTS

REFERENCES

Bruton, D.A.S., Carr, M., Crawford, M., Poiate, E. 2005. The safe design of hot on-bottom pipelines with lateral buckling using the design guideline developed by the SAFEBUCK Joint Industry Project. *Deep Offshore Technology Conference*, Vitoria, Brazil.

Bruton, D.A.S., White, D.J., Carr, M., Cheuk, J.C.Y. 2008. Pipe-soil interaction during lateral buckling and pipeline walking – the SAFEBUCK JIP. In: *Proceedings of the Offshore Technology Conference*, Houston, Texas, USA.

Bruton, D.A.S., Carr, M., Sinclair, F. 2011. Geotechnical challenges for deepwater pipeline design – SAFEBUCK JIP. *Frontiers in Offshore Geotechnics*, Gouvenec & White (Eds), London

Chee, J., Walker, A., White, D. 2018. Controlling lateral buckling of subsea pipeline with sinusoidal shape pre-deformation. *Ocean Engineering*, 151, pp.170-190.

Cumming, G., Druzynski, A., Rathbone, A. 2009. Lateral walking and feed-in of buckled pipelines due to interaction of seabed features. In: *Proceedings of the ASME 28th International Conference on Ocean, Offshore, and Arctic Engineering*, Honolulu, Hawaii, USA.

Cumming, G., Rathbone, A. 2010. Euler buckling of idealized horizontal pipeline imperfections. In: *Proceedings of the ASME 29th International Conference on Ocean, Offshore, and Arctic Engineering*, Shanghai, China.

Chee, J., Walker, A., White, D. 2018. Controlling lateral buckling of subsea pipeline with sinusoidal shape pre-deformation. *Ocean Engineering*, 151, pp.170-190.

De Leeuw, L.W., Diambra, A., Dietz, M.S., Mylonakis, G., Milewski, H. 2019. Interface shear strength of polypropylene pipeline coatings and granular materials at low stress level. In: *E3S Web of Conferences*, 92, pp.13010. EDP Sciences.

De Leeuw, L.W., Martin, G., Milewski, H., Dietz, M.S., Diambra, A. 2020a. Polypropylene pipe interface strength on marine sandy sediments of varying gravel content. *Geotechnical Engineering*, Under Review.

Endal, G., Giske, S.R., Moen, K., Sande, S. 2014. Reel-lay method to control global pipeline buckling under operating loads. In: *ASME Proceedings of the 33rd International Conference on Ocean, Offshore and Arctic Engineering*.

Jin, J., Audibert, J.M., Kan, W.C. 2010. Practical design process for flowlines with lateral buckling. In: *Proceedings of the ASME 29th International Conference on Ocean, Offshore and Arctic Engineering*, Shanghai, China.

Jukes, P., Wang, S., Wang, J. 2008. The sequential reeling and lateral buckling simulation of pipe-in-pipe flowlines using finite element analysis for deep-water applications. In: *Proceedings of the 18th International Offshore (Ocean) and Polar Engineering Conference*.

Jukes, P., Eltaher, A., Sun, J. 2009. The latest developments in the design and simulation of deepwater subsea oil and gas pipelines using FEA. In: *Proceedings of the ISOPE 3rd International Deep-Ocean Technology Symposium: Deepwater Challenge*, pp. 70-82.

Liu, R., Xiong, H., Wu, X., Yan, S. 2014. Numerical studies on global buckling of subsea pipelines. *Ocean Engineering*, 78, pp.62-72.

Milewski, H., Dietz, M.S., Diambra, A., de Leeuw, L.W. 2019. Axial resistance of smooth polymer pipelines on sand. In: *Proceedings of the ASME 38th International Conference on Offshore Mechanics and Arctic Engineering*, Glasgow, United Kingdom.

Milewski, H., Diambra, A., de Leeuw, L.W., Dietz, M.S. 2020. Axial resistance of rough pipelines on sand. In: *Proceedings of the 4th International Symposium on Frontiers in Offshore Geotechnics*, Austin, Texas, USA.

OSPAR, 2010. Quality Status Report 2010. Available online: http://qsr2010.ospar.org/en/index.html [Accessed 22nd October 2019].

Paramor, O.A.L., Allen, K.A., Aanesen, M., Armstrong, C., Hegland, T., Le Quesne, W., Piet, G.J., Raakær, J., Rogers, S., van Hal, R., van Hoof, L.J.W., van Overzee, H.M.J., Frid, C.L.J. 2009. *MEFEPO North Sea Atlas*. University of Liverpool, United Kingdom. ISBN 0 906370 60 4

Perinet, D., Frazer, I. 2006. Mitigation methods for deepwater pipeline instability induced by temperature and pressure. In: *Proceeding of the Offshore Technology Conference*, Houston, Texas, USA.

Psyrras, N., Gerasimidis, S. Kwon, O-S., Sextos, A.G. 2018. Can a buried natural gas pipeline buckle locally during earthquake ground shaking? *Soil Dynamics and Earthquake Engineering*, 116, pp.511-529.

Shadravan, A., Amani, M. 2012. HPHT 101 – What petroleum engineers and geoscientists should know about high pressure high temperature wells environment. *Energy Science and Technology*, 4 (2), pp.36-60.

Sun, J. Jukes, P., Kenny, W.G. 2011. The advancements of FEA in confronting the deepwater pipelines under high pressure and high temperature. In: *Proceedings of the Offshore Technology Conference*, Brazil.

Verley, R.L.P., Sotberg, T., 1994. A soil resistance model for pipelines placed on sandy soils. *Journal of Offshore Mechanics and Arctic Engineering*, 116 (3), pp.145-153.

Westgate, Z.J., White, D.J., Savazzi, M. 2018. Experience with interface shear box testing for axial pipe-soil interaction assessment on soft clay. *Offshore Technology Conference*.

White, D.J. and Tian, Y., 2014. Pipeline Lateral Buckling: Realistic Modelling of Geotechnical Variability and Uncertainty. *Offshore Technology Conference,* 25286